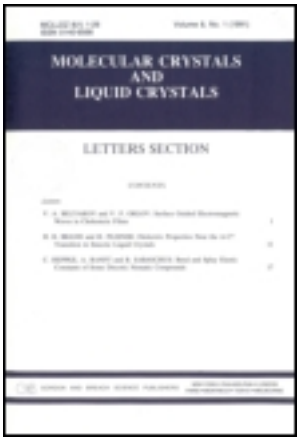

Molecular Crystals and Liquid Crystals
Publication details, including instructions for authors and subscription information:
http://www.tandfonline.com/loi/gmcl20

Solvent Dependent Energy Transfer of N-bridged Naphthalimide-Bisindolymaleimide Fluorescent Dyes

Xiaochuan Li [a], Kaijuan Zhu [a], Yajuan Li [a], Hyungjoo Kim [b] & Young-A Son [b]

[a] College of Chemistry and Environment Science, Key Laboratory of Green Chemical Media and Reactions, Ministry of Education, Henan Normal University, Xinxiang, Henan, 453007, China

[b] Department of Advanced Organic Materials Engineering, Chungnam National University, Daejeon, 305-764, Republic of Korea

Published online: 16 Dec 2013.

To cite this article: Xiaochuan Li, Kaijuan Zhu, Yajuan Li, Hyungjoo Kim & Young-A Son (2013) Solvent Dependent Energy Transfer of N-bridged Naphthalimide-Bisindolymaleimide Fluorescent Dyes, Molecular Crystals and Liquid Crystals, 584:1, 18-26, DOI: 10.1080/15421406.2013.844882

To link to this article: http://dx.doi.org/10.1080/15421406.2013.844882

Mol. Cryst. Liq. Cryst., Vol. 584: pp. 18–26, 2013

ISSN: 1542-1406 print/1563-5287 online
DOI: 10.1080/15421406.2013.844882

Solvent Dependent Energy Transfer of *N*-bridged Naphthalimide-Bisindolymaleimide Fluorescent Dyes

XIAOCHUAN LI,[1,*] KAIJUAN ZHU,[1] YAJUAN LI,[1] HYUNGJOO KIM,[2] AND YOUNG-A SON[2,*]

[1]College of Chemistry and Environment Science, Key Laboratory of Green Chemical Media and Reactions, Ministry of Education, Henan Normal University, Xinxiang, Henan, 453007, China
[2]Department of Advanced Organic Materials Engineering, Chungnam National University, Daejeon 305-764, Republic of Korea

*Double build-in chromophores, naphthalimide (**NIM**) and bisindolymaleimide (**BIM**), were synthesized and characterized. Absorption and emission properties of double chromophores dye were fully investigated in various solvents. The priority of through bond energy transfer (**TBET**) to **NTM** or **BIM** is solvent dependent. There appears large different emission wavelength change in $CHCl_3$ and DMF with alkyl attached to **BIM**. However, the product of cyclohexyl substitution leads to a different emission behavior, which is non-sensitivity to solvent polarity. Quantum chemical calculation for the molecular orbital reveals that intramolecular charge transfer (**ICT**) is the key factor for their different opto-electronic properties.*

Keywords Biindolymaleimide; ICT; naphthalimide; solvent dependent; TBET

Introduction

Research into multichromphoric energy transfer cassettes has been motivated by their promising application in organic field effect transistors, photovoltaic devices, probe, and single molecule spectroscopy [1–5]. One of the chromophore was excited by the absorption of a photon of light and then the energy transfer occurred with the donor returning to its ground state simultaneously with raising of the acceptor to its excited state. The types for the excitation energy transfer (**EET**) have two pathways: (i) through bond and (ii) through space [6–8]. The first pathway is a non-radiative energy transfer from a donor to an acceptor with conjugated bond connecting two chromophores. The second pathway requires strong overlap between the emission spectrum of the donor and absorption of the acceptor. These requirements led us design systems with two fragments twisted to each other.

In this report, two different chromophores, **NTM** and **BIM**, were incorporated together. **NTM** and **BIM** have similar maxima absorption peaks at 350–500 nm. **NTM** was a typical

*Address correspondence to Young-A Son, Department of Advanced Organic Materials and Textile System Engineering, Chungnam National University, 220 Gung-dong, Yuseong-gu, Daejeon 305-764, Korea (ROK). Tel.: (+82)42-821-6620; Fax: (+82)42-821-8870. E-mail: yason@cnu.ac.kr; or lixiaochuan@henannu.edu.cn

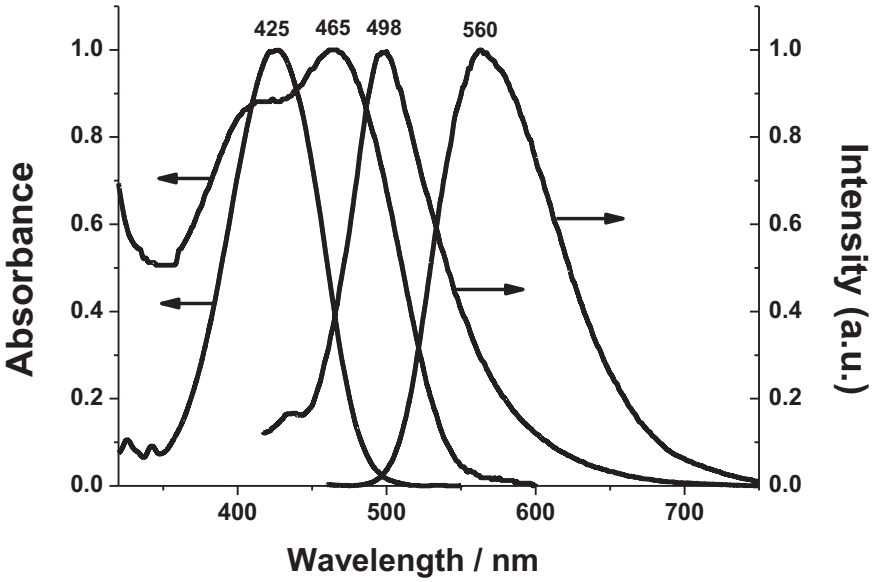

Figure 1. Spectra overlap between **NTM** emission and **BIM** absorption.

green fluorescent dye with its maximum emission at 490 nm in THF (Fig. 1) [9,10]. The longest maximum emission of **BIM** located at 560 nm. The –N– linker between the two fragments was selected, which prevent the whole molecular from becoming planar because if they did the system would behave as a single conjugated dye. Absorption of the two fragments overlaps with each other, both of which have an electron deficient heterocyclic, imide. The electron donor, —N— linker, located in the middle of **NTM** and **BIM**. Different energy transfer induced by the middle N atom depending on different environment.

Experimental

Materials

4-Bromo-1,8-naphthalic anhydride and dibromomaleimide were purchased from Aldrich. **2** (*N*-alkyl-4-bomo-1,8-naphthalimide) was synthesized following the published procedure [10–12]. The bromo atom of **2** was substituted by hydrazine hydrate and gave **3** [13]. **5** and **6** were synthesized according to our previous studying [10]. Modified synthetic procedure of **6** increased the synthetic yield greatly. All the solvents used in reaction were analytical grade and were dried according to the standard procedures. Solvents used in photochemical measurement were spectroscopic grade and purified by distillation. The stock solutions of compounds (2×10^{-3}M) were prepared, and a fixed amount of these concentrated solutions were added to each experimental solution.

Synthesis

6 (Bisindolylmaleic anhydride) was synthesized following a modified procedure according to our previous study [10,12]. **5** (0.71 g, 2 mmol) was added to 10% KOH (200 mL) and refluxed for 30 min. The reaction mixture cooled and acidified with 2N HCl. The red deposit

was collected. Aqueous was extracted by ethyl acetate (2 × 100 mL). The organic phase was dried and evaporated in vacuum. The crude product, together with the red deposit, was purified by chromatography on silica gel (EtOAc/hexane = 3:1). 667 mg red powder was obtained with 95% yield. ^{1}H NMR data of **6** was identical to previously report.

Synthesis of **NTM-BIM**s was followed by a one step procedure as shown in Scheme 1. To a magnetically stirred solution of **3** (0.1 mmol) and **6** (0.1 mmol) in absolute ethanol (10 mL) added K_2CO_3 (28 mg, 0.2 mmol). The mixture was refluxed for 12 h and monitored by TLC. When the TLC analysis revealed complete condensation, the reaction mixture was cooled to room temperature. Solvent was evaporated in vacuum. The crude product was chromatographed on silica gel (eluent: CH_2Cl_2) giving deep red solid powder.

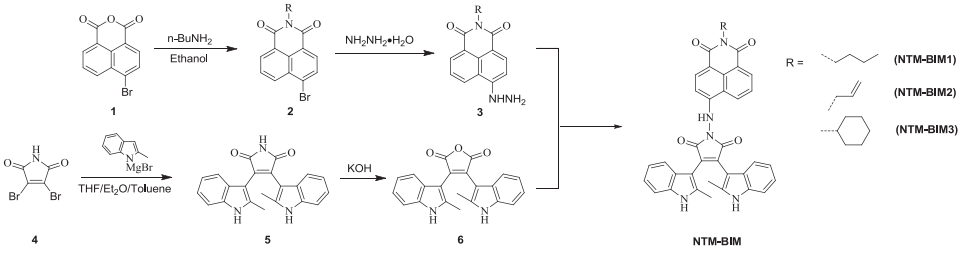

Scheme 1.

NTM-BIM1 Yield 63%; ^{1}H NMR (400 MHz, DMSO-d_6) δ 11.48 (s, 1H), 10.93 (s, 1H), 10.86 (s, 1H), 7.26 (d, J = 8.1 Hz, 2H), 7.08 (d, J = 8.0 Hz, 2H), 6.95 (dd, J = 7.5, 5.0 Hz, 3H), 6.90 (d, J = 7.6 Hz, 3H), 6.78 (dd, J = 16.2, 8.6 Hz, 3H), 4.03 (d, J = 7.1 Hz, 2H), 2.36 (t, 2H), 2.03 (s, 6H), 1.83 (m, 2H), 1.23 (m, 2H), 0.91 (t, J = 15.3, 8.3 Hz, 3H); ^{13}C NMR (100 MHz, DMSO-d_6) δ 167.7, 166.8, 162.8, 162.5, 158.6, 135.7, 135.1, 134.7, 131.9, 131.4, 130.8, 130.5, 130.1, 128.1, 127.8, 127.1, 126.6, 122.1, 122.3, 120.8, 120.5, 116.8, 115.7, 114.3, 113.6, 107.3, 106.8, 39.7, 30.1, 20.7, 16.1, 15.8, 14.0; HRMS Calcd for $C_{38}H_{31}N_5O_4$: 621.2376, found: 621.2380.

NTM-BIM2 Yield 60%; 11.48 (s, 1H), 10.86 (s, 1H), 7.26 (d, J = 8Hz, 2H), 7.20 (t, J = 8Hz, 1H), 7.07 (d, J = 8Hz, 2H), 7.02 (d, J = 8Hz, 1H), 6.99–6.94 (m, 3H), 6.90 (d, J = 8Hz, 1H), 6.79 (t, J = 8Hz, 2H), 6.73 (t, J = 8Hz, 1H), 4.03 (q, J = 8Hz, 1H), 3.60 (s, 1H), 3.55 (s, 2H), 3.51 (s, 2H), 2.36 (s, 3H), 1.83 (s, 3H); ^{13}C NMR (100 MHz, DMSO-d_6) δ 168.0, 167.1, 162.5, 161.3, 159.6, 135.3, 135.0, 134.1, 133.8, 132.0, 131.6, 131.1, 130.8, 129.0, 128.1, 127.5, 126.1, 123.8, 122.0, 121.4, 120.4, 117.2, 116.5, 115.5, 112.6, 106.1, 105.9, 41.3, 16.3, 15.6; HRMS Calcd for $C_{37}H_{27}N_5O_4$: 605.2063, found: 621.2065.

NTM-BIM3 Yield 55%; 11.47 (s, 1H), 10.85 (s, 1H), 7.26 (d, J = 8Hz, 2H), 7.19 (t, J = 8Hz, 1H), 7.07 (d, J = 8Hz, 2H), 7.02 (d, J = 8Hz, 1H), 7.99–7.93 (m, 3H), 6.90 (d, J = 8Hz, 1H), 6.79 (t, J = 8Hz, 2H), 6.73 (t, J = 8Hz, 1H), 4.06–3.97 (m, 1H), 3.59 (s, 1H), 2.36 (s, 3H), 1.83 (s, 3H), 1.56 (m, 2H), 1.35 (m, 4H), 1.27 (s, 2H), 1.21 (t, J = 8Hz, 2H); ^{13}C NMR (100 MHz, DMSO-d_6) δ 167.9, 166.9, 162.5, 162.3, 161.6, 136.9, 136.0, 135.5, 135.1, 132.8, 132.0, 131.6, 130.8, 130.3, 129.7, 128.8, 128.1, 127.6, 126.8, 125.7, 124.8, 123.3, 122.5, 120.2, 119.1 115.3, 114.1, 113.6, 107.8, 106.4, 55.9, 33.7, 31.4, 262, 24.6, 16.8; HRMS Calcd for $C_{40}H_{33}N_5O_4$: 647.2533, found: 647.2535.

Measurements

The NMR spectra were recorded on Brucker Advance 400 spectrometer, operating at 400 MHz (^{1}H) and 100 MHz (^{13}C) in DMSO-d$_6$. Mass and high resolution spectra were

measured on a LC-MS (Waters120 QTof) and Brucker microOTOF II Focus, respectively. Absorption spectra measured with PERSEE TU-1900 spectrophotometer with an external slit width of 2.5 mm used to collect absorption. Prior to the spectroscopic measurements solutions were deoxygenated by bubbling nitrogen through them.

For the theoretical study of excited states of NTM-BIMs, the *Material Studio* package was used. The ground state geometries and HOMO/LUMO frontier orbital of NTM-BIMs were calculated by LDA (local density approximation) methods at the PWC (Perdew-Wang functional) level.

Results and Discussion

The UV-vis absorption and emission spectra of **NTM-BIM**s are measured in various solvents of different polarity. Figure 2 shows the typical absorption spectra of **NTM-BIM**s in THF (1×10^{-5}M). Three compounds exhibit very similar absorption contour outline. The absorption bands cross over 350–600 nm with continuously decreased tendency. Only an absorption platform appears around 340 nm. It indicates that there are significant electronic coupling between naphthalimide and bisindolylmalimide entities in the ground state.

Emission spectra of **NTM-BIM**s in various solvent of different polarity exhibit distinctly different emission behavior. Because of poor solubility in hexane, the emission behavior in hexane was not investigated. In polar DMF, exciting **NTM-BIM3** at 365 nm provides an emission of 455 nm. The emission from **BIM** moiety is almost quenched completely. In contrast, the emission from **NTM** moiety is observed at 540 nm for **NTM-BIM1** and 520 nm for **NTM-BIM2**, respectively. Whereas the fluorescence spectra of a 1:1 mixture of **NTM** and **BIM** exhibit dual emission bands at 498 nm and 560 nm. It should be noted that the emission of **NTM-BIM3** in DMF blue-shifted 40 nm compared with that of **NTM**. Figure 3(c) shows that variation of the solvent polarity does not induce significant emission shift for **NTM-BIM3**. The maxima emission wavelength varied from 444 nm to 455 nm. For **NTM-BIM1** and **NTM-BIM2**, variation of solvent polarity induces significant change of maxima emission wavelength. In $CHCl_3$, maxima emission

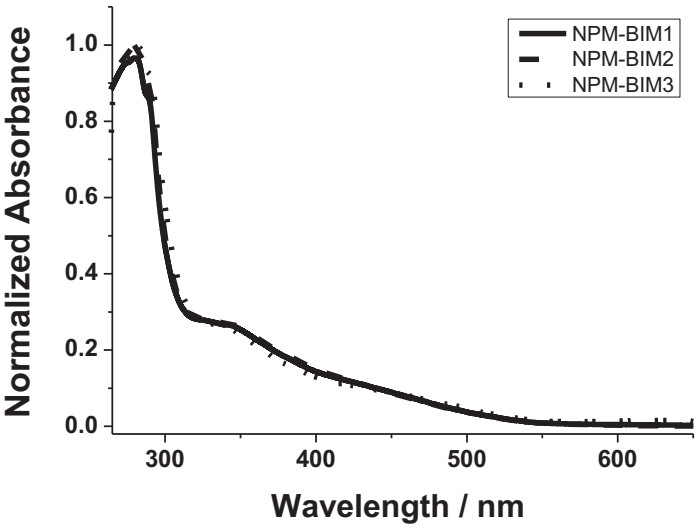

Figure 2. UV-vis absorption spectra of compounds **NTM-BIM**s (1.0×10^{-5} M) in THF.

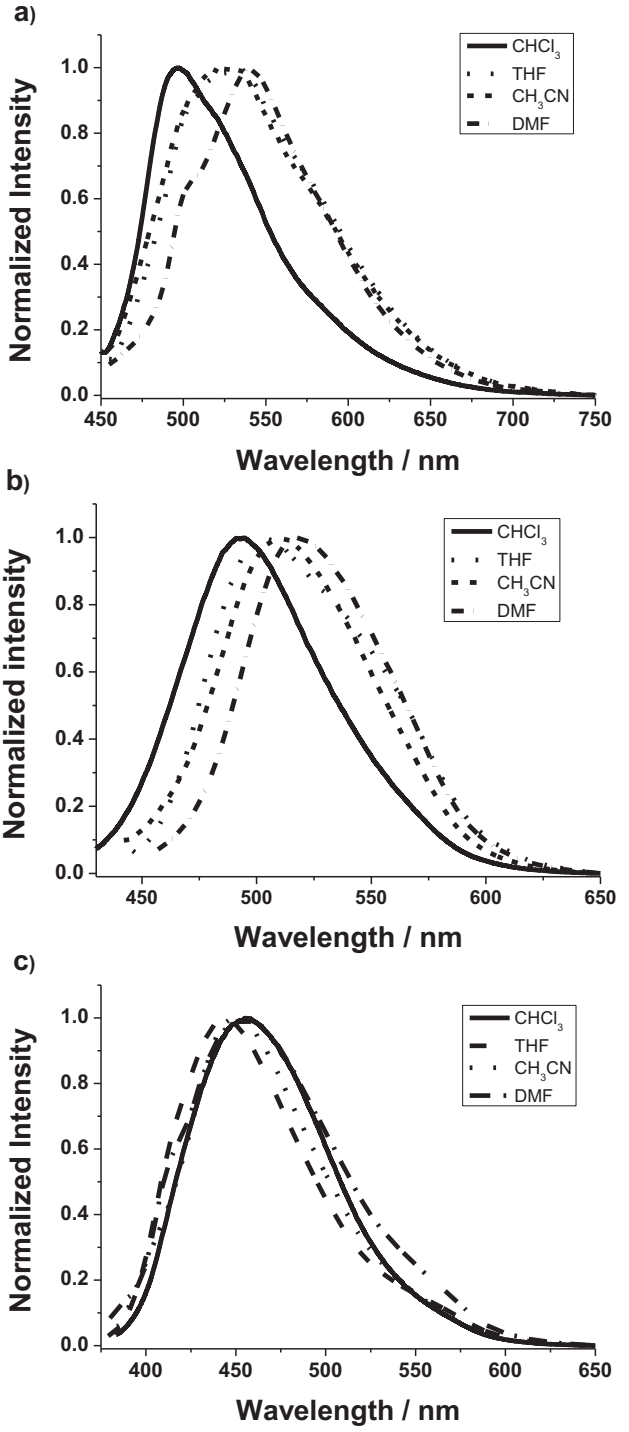

Figure 3. Fluorescence emission spectra of **NTM-BIM**1 (a), **NTM-BIM**2 (b), and **NTM-BIM**3 (c) in $CHCl_3$, THF, CH_3CN, and DMF.

of **NTM-BIM1** and **NTM-BIM2** are centered at 496 nm and 493 nm, respectively. The emission from **BIM** moiety is quenched completely. These results indicate that solvent polarity changing can induce different **TBET** direction with alkyl substituting on the top of **BIM** moiety. However, this solvent polarity induced **TBET** direction is suppressed with cyclohexyl substitution on the top of **BIM** moiety, in which only the **TBET** from **BIM** to **NTM** observed. The fluorescence quantum yield of each compound was determined in $CHCl_3$ with reference to quinine bisulfate in 0.05M H_2SO_4 aqueous solution ($\Phi = 0.51$). The fluorescence quantum yield of the three dyes in different solvent ranged from 0.18 to 0.26.

All the **NTM-BIM**s exhibit large stokes shift. In $CHCl_3$, the Stokes shifts of **NTM-BIM1** and **NTM-BIM2** were estimated to be 131 nm with 365 nm excitation. However, the Stokes shift of **NTM-BIM3** is only 84 nm (372 nm excitation). In DMF, the Stokes shift for **NTM-BIM1** and **NTM-BIM2** also up to 114 nm and 96 nm, respectively. For **NTM-BIM3**, the Stokes shift is 85 nm in DMF, which is almost identical to that in $CHCl_3$. It has been clear that red-shifted emission does not necessarily induce a large Stokes shift because the two photophysical parameters are of entirely different origin [14,15]. In principle, the emission wavelength of fluorophore is related to the size of π-conjugation or the **ICT** feature of the fluorophore [16]. For the Stokes shift, the geometry relaxation at the S_1 state after vertical excitation from S_0 state is crucial.

According to the mentioned above, **NTM-BIM3** is not sensitive to solvent polarity. Emission wavelength of it is independent of the solvent polarity, although the emission intensity decreased in more polar solvents, such as DMF. The Stokes shift around 84 nm is an intrinsic property, not a solvent-polarity induced phenomena, or any **ICT** related results. The fluorescence of **NTM-BIM1** and **NTM-BIM2** in $CHCl_3$ exhibited blue emission. However, light green emission was observed in DMF. The emission changed from blue to light green together with the large Stokes shift will be useful for the dyes in fluorescent molecular probes or intracellular fluorescent bio-imaging.

Figure 4 shows the solid-state emission of **NTM-BIM**s. The solid powder of **NTM-BIM1** and **NTM-BIM2** exhibits bright orange color with 365 nm excitation. **NTM-BIM3**

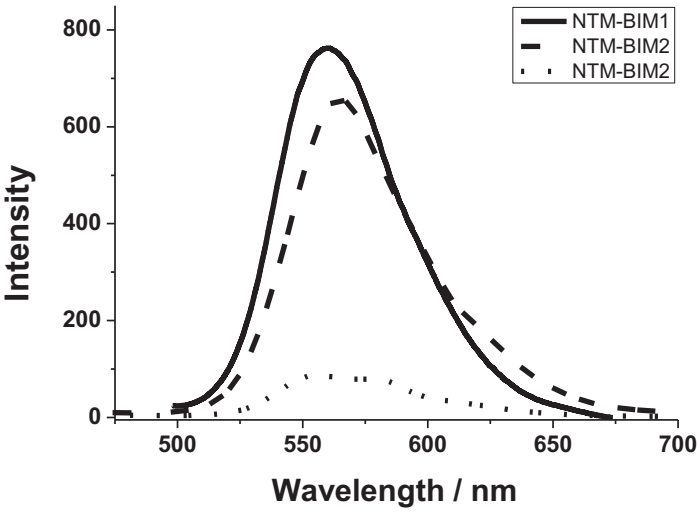

Figure 4. Fluorescence spectra in solid state of **NTM-BIM**s.

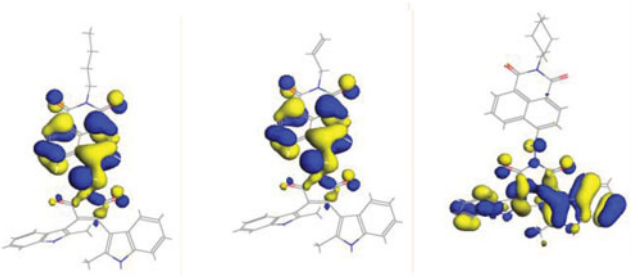

Figure 5. Representative HOMO-1 diagrams of **NTM-BIM**s obtained from *Dmol*[3] calculations.

is a dark red powder with very weak emission in solid state. The full width at half maximum for **NTM-BIM1** and **NTM-BIM2** are 59 nm and 58 nm, respectively. The narrow solid-state emission bands of **NTM-BIM1** and **NTM-BIM2** are unusual and intriguing, as spectral broadening is a very common phenomenon for solid emitting materials. The alkyl attached on **NTM**, which to some extent, prevents the molecules from packing compactly and thus avoids the spectral broadening. Few intermolecular interactions between molecules provide favorable factors that eliminate self-quenching and enhance their solid fluorescence.

To gain insights into the nature of electronic transitions of these dyes, molecular orbital (**MO**) and optimization of molecular structure were carried out on the density function theory (DFT) level using LDA/PWC basis set as implement in the *Dmol*[3] package [17,18]. Distinctive contributions of each atomic orbital are discernible in the MO diagrams. Figure 5 shows the representative HOMO-1 diagrams of **NTM-BIM**s. An obvious different electron density distribution can be observed between **NTM-BIM1/ NTM-BIM2** and **NTM-BIM3**. For **NTM-BIM1/NTM-BIM2**, the electron density in the HOMO-1s is well-distributed over the **NTM** ring. In contrast, the electron density distribution in HOMO-1 for **NTM-BIM3** is contributed mainly from the indole and maleimide moiety. HOMOs/LUMOs of the three dyes are almost identical to each other, and a representative HOMO and LUMO is showed in Fig. 6. There appears to be a regular trend in the HOMOs and LUMOs for **NTM-BIM**s. In HOMOs, electron spread over the two indole rings and maleimide ring, whereas the electron centralizes on maleimide moiety in LUMOs. It is clearly indicated

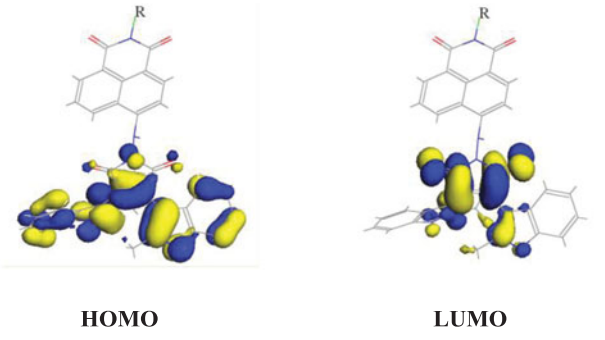

Figure 6. Typical representative HOMO and LUMO diagram of **NTM-BIM**s. R = substituted butyl, allyl, and cyclohexyl group.

that effective charge transfer states in acceptor-donor-acceptor molecular systems of **NTM-BIM1/NTM-BIM2**, which leads to the sensitivity to the solvent polarity. Without the effective charge transfer in **NTM-BIM3**, very weak sensitivity to the solvent polarity was observed.

Conclusions

Acceptor-donor-acceptor molecular system with different chromophores, NTM and BIM, was designed and synthesized. Its opto-physical properties were fully investigated in different solvent polarity. The experimental results showed that different solvent could induce different excited state energy transfer direction for **NTM-BIM1/NTM-BIM2**. This phenomenon typically occurred in $CHCl_3$ and DMF. In $CHCl_3$, the maximum emission located around 490 nm. However, the maximum emission wavelength shifted over to 520 nm in DMF. Interestingly, this trend was suppressed for **NTM-BIM3** without effective delocalization of electrons like **NTM-BIM1/NTM-BIM2**. **NTM-BIM1/NTM-BIM2** also exhibit bright solid-state emission with narrow emission bands (fwhm: 58 nm and 59 nm). These properties, especially for **NTM-BIM1/NTM-BIM2** qualify them as multifunctional fluorophores with potential application in light-emitting or –sensing devices. Further investigation, together with newly designed molecules, along those lines is in progress.

Acknowledgments

This work was supported by the National Natural Science Foundation of China (grant no. 21072048), the PIRTUHP (grant no. 2012IRTSTHN006), PCSIRT (grant no. IRT1061), and by the Basic Science Research Program through the National Research Foundation of Korea (NRF) funded by the Ministry of Education, Science and Technology (grant no. 20120008198).

References

[1] Albers, A. E., Okreglak, V. S., & Chang, C. J. (2006). *J. Am. Chem. Soc*., *128*, 9640.
[2] Chen, X., Pradhan, T., Wang, F., Kim, J. S., & Yoon (2012). *J. Chem. Rev.*, *112*, 1910.
[3] Maeda, T., Hamamura, Y., Miyanaga, K., Shima, N., Yagi, S., & Nakazumi, H. (2011). *Org. Lett*., *13*, 5994.
[4] Huang, J., Luo, H., Wang, L., Guo, Y., Zhang, W., Chen, H., Zhu, M., Liu, Y., & Yu, G. (2012). *Org. Lett*., *14*, 3300.
[5] Shcherbakova, D. M., Hink, M. A., Joosen, L., Gadella, T. W. J., & Verhhusha, V. V. (2012). *J. Am. Chem. Soc*., *134*, 7913.
[6] Jiao, G. -S., Thoresen, L. H., & Burgess, K. (2003). *J. Am. Chem. Soc*., *125*, 14668.
[7] Lin, W., Yuan, L., Cao, Z., Feng, Y., & Song, J. (2010). *Angew. Chem. Int. Ed*., *49*, 375.
[8] Lin, W., Yuan, L., Long, L., Guo, C., & Feng, J. (2008). *Adv. Funct. Mater.*, *18*, 2366.
[9] Veale, E. B., & Gunnlaugsson, T. (2010). *J. Org. Chem*., *75*, 5513.
[10] Li, X., Chen, J., Ma, D., Zhang, Q., & Tian, H. (2005). *Proc. of SPIE*, *5632*, 357.
[11] Li, Y., Cao, L., Ning, Z., Huang, Z., Cao, Y., & Tian, H. (2007). *Tetrahedron Lett*., *48*, 975.
[12] Li, X., Xu, Y., Wang, B., & Son, Y. (2012). *Tetrahedron Lett*., *53*, 1098.
[13] Gan, J., Tian, H., Wang, Z., Cheng, K., Hill, J., Lane, P. A., Rahn, M. D., Fox, A. M., & Bradley, D. D. C. (2002). *J. Organomet. Chem. 645*, 168.

[14] Lakowicz, J. R. (1999). *Principles of Fluorescence Spectroscopy*, Kluwer Academic: New York.
[15] Valeur, B. (2001). *Molecular Fluorescence: Principles and Application*, Wiley-VCH Verlag GmbH: Weinheim.
[16] Rachford, A. A., Ziessel, R., Bura, T., Retailleau, P., Castellano, F. N. (2008). *Org. Lett.*, *10*, 1581.
[17] Delley, B. (1990). *J. Chem. Phys.*, *92*, 508.
[18] Delley, B. (2000). *J. Chem. Phys.*, *113*, 7756.